Actin polymerization as a novel innate immune effector mechanism to control *Salmonella* infection

Si Ming Man[1†], Andrew E. Ekpenyong[2,3†], Panagiotis Tourlomousis[1], Sarra Achouri[2], Eugenia Cammarota[2], Katherine Hughes[1], Alessandro Rizzo[2], Gilbert Ng[2,3], John A. Wright[1], Pietro Cicuta[2], Jochen Guck[2,3], Clare E. Bryant*[1]

[1]Department of Veterinary Medicine, University of Cambridge, Madingley Road, Cambridge CB3 0ES, UK

[2] Sector of Biological and Soft Systems, Cavendish Laboratory, University of Cambridge, JJ Thomson Avenue, Cambridge CB3 0HE, UK.

[3]Biotechnology Center, Technische Universität Dresden, Tatzberg 47/49, 01307 Dresden, Germany.

* Correspondence to: C.E. Bryant (ceb27@cam.ac.uk)
Department of Veterinary Medicine,
University of Cambridge,
Madingley Road, Cambridge CB3 0ES, UK.

† These authors contributed equally to this work.

Keywords: Inflammasome, actin, cytoskeleton, NLRC4, NLRP3, NLRs, ASC, caspase-1, caspase-11, IL-1, *Salmonella*, bacteria, pathogen, infection, immunity, infectious diseases, cell stiffness

Abbreviations: ASC, Apoptosis-associated speck-like protein containing a CARD; NLRs, nucleotide-binding domain and leucine-rich repeat containing family; NLRP3, nucleotide-binding domain and leucine-rich repeat containing family, pyrin domain–containing 3, NLRC4, nucleotide-binding domain and leucine-rich repeat containing family, CARD domain–containing 4; ROS, reactive oxygen species; SCV, *Salmonella*-containing vacuole; TLRs, Toll-like receptors; WT, wild type.

The authors declare no competing conflict of interest.

ABSTRACT

Salmonellosis is one of the leading causes of food poisoning worldwide. Controlling bacterial burden is essential to surviving infection. Nucleotide-binding oligomerization domain-like receptors (NLRs), such as NLRC4, induce inflammasome effector functions and play a crucial role in controlling *Salmonella* infection. Inflammasome-dependent production of interleukin-1β (IL-1β) recruits additional immune cells to the site of infection, while inflammasome-mediated pyroptosis of macrophages releases bacteria for uptake by neutrophils. Neither of these functions is known to directly kill intracellular salmonellae within macrophages. The mechanism, therefore, governing how inflammasomes mediate intracellular bacterial killing and clearance in host macrophages remains unknown. Here, we show that actin polymerization is required for NLRC4-dependent regulation of intracellular bacterial burden, inflammasome assembly, pyroptosis and IL-1β production. NLRC4-induced changes in actin polymerization are physically manifested as increased cellular stiffness, and leads to reduced bacterial uptake, production of antimicrobial molecules and arrested cellular migration. These processes act in concert to limit bacterial replication in the cell and dissemination in tissues. We show, therefore, a functional link between innate immunity and actin turnover in macrophages that underpins a novel host defense mechanism for the control of salmonellosis.

SIGNIFICANCE STATEMENT

Infectious diseases are responsible for one-third of all mortality worldwide. Innate immunity is critical for mounting host defenses that eliminate pathogens. *Salmonella* is a global foodborne pathogen that infects and replicates within macrophages. How inflammasomes – multi-meric protein complexes that provide innate immune protection – function to restrict bacterial burden in macrophages remains unknown. We show that actin polymerization is critical for NLRC4 inflammasome activation in response to *Salmonella* infection. NLRC4 activation in *Salmonella*-infected cells prevents further uptake of bacteria by inducing cellular stiffness and antimicrobial responses, which prevent bacterial dissemination in the host. These results demonstrate a critical link between innate immunity and the actin cytoskeleton in the cellular defense against *Salmonella* infection.

\body

INTRODUCTION

A critical step in disease pathogenesis for many clinically important bacteria is their ability to infect and survive within host cells such as macrophages. *Salmonella enterica,* a pathogen which resides and replicates within macrophages, causes a range of life-threatening diseases in humans and animals, and accounts for 28 million cases of enteric fever worldwide each year (1). *S. enterica* infects phagocytes by a process that requires cytoskeletal reorganization (2). This bacterium resides in a *Salmonella*-containing vacuole (SCV) within host macrophages. This intracellular lifestyle enables them to avoid extracellular antimicrobial killing, evade adaptive immune responses and potentially to spread to new sites to seed new infectious foci within host tissue, which eventually develop into granulomas (3). Survival and growth of *S. enterica* within phagocytes is critical for virulence (4) and host restriction of the intracellular bacterial load is, therefore, paramount in surviving salmonellosis. *Salmonella* delivers microbial effector proteins into the host cell via the type III secretion systems (T3SS), mediated by the *Salmonella* pathogenicity island-1 and -2 (SPI-1 and SPI-2), to subvert cellular functions and facilitate intracellular survival (5).

Microbes are recognized by macrophages through pattern recognition receptors (PRRs), such as Toll-like receptors (TLRs) and nucleotide-binding oligomerization domain-like receptors (NLRs), which initiate innate immune responses, including cytokine production and pathogen killing (6). NLRs drive the formation of inflammasomes – macromolecular protein complexes – comprising one or more NLRs, usually an adaptor protein (ASC) and the effector protein caspase-1, which then cleaves pro-interleukin-1β (IL-1β) and pro-IL-18 into biologically active cytokines, and initiates macrophage cell death by pyroptosis (7). NLRC4, in concert with NAIPs

1, 2, 5 and 6, is a key PRR that forms an inflammasome complex upon sensing flagellin and/or the inner rod or needle proteins (PrgJ and PrgI, respectively) of the SPI-1 T3SS of *S. enterica* serovar Typhimurium (*S.* Typhimurium) (8-11). Activation of the NLRC4 inflammasome by *Salmonella* infection results in IL-1β and IL-18 production driven by an ASC-dependent pathway and macrophage pyroptosis driven by an ASC-independent pathway (12, 13). A second, non-canonical, NLR signaling pathway has been described, which requires caspase-11 to initiate delayed cell death and NLRP3 inflammasome activation (14-16). Effective clearance of *Salmonella* infection in host cells may therefore require a coordinated effort between different inflammasome signaling pathways.

We, and others, have shown that NLRC4 is important in regulating bacterial burden of *S.* Typhimurium *in vivo* (17-19). A recent study revealed that *Salmonella*-infected epithelial cells are extruded from the intestinal epithelium in a process which requires NLRC4 (20). The molecular mechanism behind how NLRC4 restricts bacterial burden in macrophages infected with *Salmonella* is however still unknown. Here, we identify an actin-dependent mechanism that controls NLRC4–mediated regulation of bacterial replication in macrophages infected with *S.* Typhimurium. Activation of NLRC4 in infected macrophages mediates the production of ROS to inhibit bacterial replication and limits additional bacterial uptake by inducing mechanical stiffening the cell via actin polymerization. Overall, we describe a novel effector mechanism, governed by actin and the NLRC4 inflammasome, to control *Salmonella* infection in macrophages.

RESULTS

The NLRC4 inflammasome controls intracellular bacterial numbers in macrophages

NLRC4 and NLRP3 inflammasomes are critical in controlling *Salmonella* infection *in vivo* (17-19), however, whether inflammasomes regulate intracellular bacterial load in macrophages is unknown. To investigate whether NLRC4 or NLRP3 regulate the burden of salmonellae in macrophages, we infected primary bone marrow-derived macrophages (BMMs) from WT, *Nlrc4*$^{-/-}$, *Nlrp3*$^{-/-}$, *Asc*$^{-/-}$, *Casp1*$^{-/-}$ or *Casp11*$^{-/-}$ mice with a SPI-1-competent *S.* Typhimurium (MOI 1) and quantified the number of bacteria using gentamicin protection assays. After 2 h of infection, we found a significantly higher *Salmonella* burden in *Nlrc4*$^{-/-}$ or *Casp1*$^{-/-}$ BMMs compared to WT BMMs (**Fig. 1A**). The *Casp1*$^{-/-}$ mouse strain was recently shown to be deficient in caspase-11 (herein referred to as *Casp1/11*$^{-/-}$) (14). *Casp11*$^{-/-}$ BMMs infected with *S.* Typhimurium, however, contained similar number of bacteria compared to WT BMMs (**Fig. S1**), indicating that caspase-1, rather than caspase-11, controls bacterial numbers in macrophages at this time point. Confocal microscopy was performed on individual macrophages infected with a GFP-expressing strain of *S.* Typhimurium and the bacterial load per cell was enumerated. A higher number of bacteria per cell was found in *Nlrc4*$^{-/-}$ and *Casp1/11*$^{-/-}$ BMMs (most had 4 – 6 bacteria per cell) compared to WT cells (most had 1 – 2 bacteria per cell; **Fig. 1B**). These results indicate that the NLRC4-caspase-1 axis restricts bacterial numbers in macrophages.

We further confirmed these results by infecting WT BMMs with isogenic mutants of *S.* Typhimurium lacking NLRC4 activators (Δ*fliC*Δ*fljB* (deletion of flagellin proteins) and Δ*prgJ*). We found that WT BMMs failed to restrict bacterial numbers in the absence of NLRC4 activation (**Fig. 1C**). Gentamicin protection assays and single cell analysis of *Salmonella*-infected *Asc*$^{-/-}$ or *Nlrp3*$^{-/-}$ BMMs revealed similar total numbers and distribution of bacteria per cell when compared to WT BMMs (**Fig. 1A and B**). Together, these results suggest that the

NLRC4 inflammasome regulates *Salmonella* burden in macrophages via a mechanism that is independent of ASC.

NLRC4 restricts bacterial replication in the *Salmonella*-containing vacuole

An elevated intracellular bacterial burden could occur by one or more of the following mechanisms: increased infection rate of macrophages, increased intracellular bacterial growth rate, or suppression of intracellular bacterial killing (21). When *S.* Typhimurium enters a macrophage, the cell must be able to limit bacterial replication to prevent overwhelming infection. The increased number of bacteria per cell in *Nlrc4*$^{-/-}$ BMMs suggests a role for NLRC4 in the inhibition of intracellular bacterial survival (**Fig. 1**). *S.* Typhimurium survive and replicate intracellularly in macrophages within SCVs of a diameter of 3 – 4 μm (**Fig. S2**). We used live confocal imaging to record the number of bacteria in each SCV over time and calculated the bacterial growth rate within each SCV from WT (n=11) and *Nlrc4*$^{-/-}$ (n = 30) BMMs over 17 h. In WT BMMs that were not killed by pyroptosis, the bacterial growth rate in the SCV was 0.12 division per hour. Bacteria in the SCVs of *Nlrc4*$^{-/-}$ BMMs, in contrast, grew twice as fast – at a rate of 0.24 division per hour (**Fig. 2A**). These results indicate that *Nlrc4*$^{-/-}$ BMMs fail to effectively restrict bacterial replication in the SCV. Effective control of intracellular *Salmonella* by macrophages has been shown to be mediated by mitochondrial ROS (mROS) activity and hydrogen peroxide produced within the cell (22). We measured mROS activity and cellular hydrogen peroxide production in BMMs infected with *S.* Typhimurium for 30 min and found that WT BMMs generated mROS activity and hydrogen peroxide after infection with *S.* Typhimurium, whereas *Nlrc4*$^{-/-}$ or *Casp1/11*$^{-/-}$ BMMs failed to induce mROS or hydrogen peroxide (**Fig. 2 B and C**). *Nlrp3*$^{-/-}$ BMMs produced mROS and hydrogen peroxide

at a level comparable to WT BMMs (**Fig. 2 B and C**), indicating that NLRC4, but not NLRP3, induces ROS in macrophages in response to *Salmonella* infection. Furthermore, inhibition of ROS in BMMs with *N*-Acetyl-l-cysteine resulted in a significantly increased number of intracellular bacteria compared to untreated controls following 2 and 6 h of infection ($P = 0.007$ for 2 h and $P = 0.013$ for 6 h; **Fig. 2D**). These results collectively demonstrate that NLRC4 contributes to the restriction of bacterial replication in SCVs.

NLRC4 modifies actin polymerization to activate inflammasome responses to *Salmonella* infection

Our live cell imaging experiments using confocal microscopy revealed important differences in the growth rate of bacteria in WT and *Nlrc4*$^{-/-}$ macrophages. To further investigate the dynamics of the infection process, we used live cell imaging to track and quantify infection events of individual WT and *Nlrc4*$^{-/-}$ macrophages infected with *S.* Typhimurium-GFP (MOI of 10) every 60 s for 1 h. WT BMMs were susceptible to infection for the first 10 min, but susceptibility to infection plateaued after 10 min, whereas *Nlrc4*$^{-/-}$ BMMs were initially less susceptible to infection compared to WT BMMs (0 – 30 min), but remained readily susceptible to infection over time (**Fig. 3A**). The failure to limit bacterial uptake in the absence of NLRC4 ultimately resulted in a greater number of total infection events per macrophage after 1 h of infection (6.8 ± 1.0 bacteria per *Nlrc4*$^{-/-}$ BMMs vs. 5.0 ± 0.7 bacteria per WT BMMs).

Cytoskeletal rearrangement, particularly changes in actin conformation, is an important process for entry of *Salmonella* into epithelial cells (23), however, it is unknown whether NLRC4 regulates cytoskeletal function to control infection in macrophages. We hypothesized that NLRC4 might alter cytoskeletal function to reduce bacterial uptake in macrophages. Inhibition

of host cell actin polymerization and reduced actin availability, using cytochalasin D (24, 25), significantly impaired *Salmonella* uptake into macrophages, whereas colchicine (a microtubule polymerization inhibitor) failed to significantly inhibit bacterial uptake after 2 h of infection (**Fig. 3B**). Cytochalasin D also dose-dependently inhibited *Salmonella*-induced NLRC4-dependent pyroptosis (**Fig. 3C**).

NLRC4 is unusual amongst the inflammasome forming NLRs in that it can activate caspase-1 directly by CARD-CARD domain interactions as well as through association with the adaptor protein ASC (26, 27). Our data suggest that changes in actin polymerization are an important effector mechanism for NLRC4-dependent ASC-independent anti-microbial effects induced by the cell, and we wondered whether this would also be true for ASC-dependent NLRC4 inflammasome activation by *S.* Typhimurium. Inflammasome activation drives the formation of a large macromolecular complex, or 'speck', within the cell whereby ASC forms the platform for recruitment of effector proteins in response to *Salmonella* infection (17, 28). We infected BMMs with *S.* Typhimurium and immunolocalized ASC at different time-points and observed the formation of an ASC speck within 5 min post-infection (**Fig. S3**). The formation of macromolecular protein complexes can be facilitated by cytoskeletal reorganization. We found that cytochalasin D, but not colchicine, inhibited the formation of these rapidly induced ASC inflammasome specks in *Salmonella*-infected BMMs (**Fig. 3D**). ASC speck formation is critical for the production of IL-1β and in our experiments cytochalasin D indeed dose-dependently blocked early NLRC4-dependent *Salmonella*-induced IL-1β production, whereas colchicine did not dose-dependently inhibited *Salmonella*-induced IL-1β production (**Fig. 3E**). We further confirmed these results and found that cytochalasin D, but not colchicine, inhibited flagellin-induced ASC speck formation and IL-1β secretion in BMMs (**Fig. S4 A and B**). These results

suggest that actin polymerization provides a mechanism by which NLRC4 activates innate immunity in response to *S*. Typhimurium.

Activation of NLRC4 modulates macrophage deformability and movement

We hypothesized that NLRC4-dependent changes in actin polymerization should impact on cytoskeletal functions within the cell. To investigate this, we used an optical stretcher, an established biophysical instrument (29), to determine whether there is a dynamic change in the cytoskeletal function of WT and *Nlrc4*$^{-/-}$ BMMs in response to *Salmonella* infection. The optical stretcher employs two counter-propagating laser beams to trap and deform individual macrophages and measure changes in their deformability or compliance (the inverse of stiffness), which is dependent on the functionality of the cytoskeleton (**Fig. 4A**) (30). When coupled to a fluorescence detector it is possible to trap and specifically stretch cells which had been infected with GFP-expressing *S*. Typhimurium. We analyzed uninfected WT or *Nlrc4*$^{-/-}$ BMMs or BMMs infected with *S*. Typhimurium-GFP at an MOI of 10 for 10 min using the optical stretcher. The BMMs were trapped, stretched for 4 s, followed by quantification of their compliance. We found that uninfected WT or *Nlrc4*$^{-/-}$ BMMs exhibited identical viscoelastic properties. Infected WT BMMs, however, exhibited a change in their viscoelastic properties, such that the macrophages became less deformable or stiffer compared to uninfected WT cells (**Fig. 4B**). Remarkably, *Nlrc4*$^{-/-}$ BMMs infected with *S*. Typhimurium showed little change in cell compliance, indicating that infection-induced cell stiffening did not occur (**Fig. 4B**).

We further confirmed the impact of NLRC4 on actin functionality with the use of phalloidin staining and three-dimensional microscopy to reconstruct the F-actin cytoskeleton to visualize actin re-organization in response to *Salmonella* infection. In WT immortalized BMMs infected

with a strain of *S.* Typhimurium expressing GFP at an MOI of 10, F-actin formed a dense network, indicated by the intense red staining around the bacterium at 5 min post-infection (**Fig. 4C**). *Nlrc4*$^{-/-}$ immortalized BMMs infected with *S.* Typhimurium showed diffused actin staining proximal to the bacteria, which failed to form a striking stranded pattern observed in WT cells (**Fig. 4C**). This process could result in a localized "stiff" region to limit the size of the SCV and may restrict bacterial growth.

A consequence of cytoskeletal rearrangements that lead to increased cell stiffness can be impaired cellular movement (31). To investigate whether *Salmonella*-induced cellular stiffness mediated by NLRC4 affects macrophage migration, we tracked the movement of uninfected primary WT and *Nlrc4*$^{-/-}$ BMMs for 3 h prior to infection and for the first 30 min post-infection. Both WT and *Nlrc4*$^{-/-}$ BMMs moved freely prior to infection (**Fig. 4D; Movie S1**). Following infection with *S.* Typhimurium, the movement of WT BMMs ceased rapidly, whereas the movement of *Nlrc4*$^{-/-}$ BMMs was unaffected, despite the increasing intracellular bacterial burden (**Fig. 4D; Movie S1**). Our data therefore suggest that *Salmonella* infection activates the NLRC4 inflammasome to cause major cytoskeletal reorganization in macrophages, reducing macrophage movement and susceptibility to infection. To confirm the physiological relevance of cellular movement in the control of salmonellosis, we performed histological analysis of liver tissue sections to investigate the number of infectious foci (lesions or granulomas induced by *Salmonella* and macrophage recruitment (3)) from mice infected with *S.* Typhimurium. An increased in bacterial burden is associated with an increase in lesion number (3). We saw an increase in bacterial burden and the number of infectious foci in *Nlrc4*$^{-/-}$ mice compared to WT mice (**Fig. 4E and F** and **Fig. S5**). Taken together, our results suggest that NLRC4 activation by *Salmonella* infection changes cytoskeletal dynamics and leads to important physiological

functions, including reduced cellular movement, suppression of bacterial uptake, and production of antimicrobial molecules, which together, leads to a reduced intracellular bacterial burden that can be effectively cleared by the cell.

DISCUSSION

Inflammasome activation provides host protection against infectious agents. The NLRC4 inflammasome is activated in response to *Salmonella* infection, inducing caspase-1-dependent cleavage and release of bioactive IL-1β and IL-18 and pyroptosis. Pyroptosis of macrophages leads to release of bacteria for uptake by other cell types such as neutrophils, but also permits bacterial dissemination (18). Neutrophils, for example, do not undergo NLRC4-mediated pyroptosis and provide a major source of IL-1β during *Salmonella* infection (32), which indicates that pyroptosis is not always required for the control of pathogen burden. Here, we have shown that macrophages that resist pyroptosis can directly control and restrict intracellular salmonellae. *Salmonella*-induced NLRC4 inflammasome activation is intimately linked to actin polymerization, where F-actin filaments are recruited to the bacteria within 5 min of infection. Efficient reorganization of the actin cytoskeleton is required for rapid ASC speck formation, a hallmark of inflammasome assembly (17, 28), which occurs within 5 min of infection.

Mechanical correlates of actin reorganization can be measured using an optical stretcher, which determines the dynamic change of the cytoskeleton and changes in its compliance. We found that *Salmonella* infection and activation of the NLRC4 inflammasome induces cellular stiffness in macrophages such that the cell has an impaired ability to take up more bacteria. This finding raises the question of whether limiting the uptake of bacteria in a cell is of benefit to the host.

Host macrophages infected by *Salmonella* may direct their resources to killing the residing bacteria prior to uptake of more bacteria. This strategy may avoid overwhelming infection, thereby, allowing more effective clearance of a small number of intracellular bacteria at a time and to avoid pyroptosis. Importantly, we found that activation of the NLRC4 inflammasome is required for generating ROS and restrict intracellular bacterial replication in the SCV.

Bacterial uptake concomitantly induces cell stiffness and impairs cellular movement. The use of actin to target and surround the invading bacteria may also reduce the total amount of actin available for cellular movement, which reduces macrophage migration and dissemination of infected cells to other areas of the tissue. Indeed, mice lacking NLRC4 exhibit increased numbers of infectious foci in liver tissues and are more susceptible to salmonellosis. A previous study has identified that β-actin and γ-actin are targets for caspase-1 cleavage (33). It is possible that *Salmonella*-induced NLRC4 inflammasome activation drives cleavage and modification of actin to arrest cellular movement. Inflammasome-induced cellular stiffening and arrest may represent a general mechanism for the control of intracellular bacterial infection. Earlier work showed that $CD4^+$ T lymphocytes infected with *Shigella flexneri* exhibit an impaired ability to migrate *in vitro* and *in vivo* (34, 35). *Shigella* can drive inflammasome activation through both NLRC4 and NLRP3 (36, 37), but it remains to be determined whether increased cell stiffness and impaired movement in immune cells are a consequence of inflammasome activity induced by pathogens other than *Salmonella* such as *Shigella* or *Listeria*. In conclusion, our work has identified a novel cellular mechanism driven by the NLRC4 inflammasome and actin polymerization to reduce intracellular *Salmonella* burden in macrophages. The fate of a macrophage and the bacterium, therefore, depends on the host-microbial engagement of the

NLRC4 inflammasome, which is governed by the number of bacteria that infect and are taken up by the cell, and the ability of the bacteria to replicate or resist bacterial killing.

MATERIALS AND METHODS

Bacterial strains. *S.* Typhimurium strain SL1344 and *S.* Typhimurium SL1344 Δ*fliC*Δ*fljB*Δ*prgJ* and the GFP-expressing strain JH3016 were used and were described previously (17, 38).

Fluorescence and confocal microscopy and analysis. To investigate the number of bacteria per macrophage, primary BMMs were infected with *S.* Typhimurium JH3016 (38), a derivative of SL1344 that expresses green fluorescent protein (GFP), for 1 h, followed by gentamicin treatment (50 μg/ml) for 1 h to kill extracellular bacteria. BMMs were washed twice with PBS, fixed in 4% (wt/vol) paraformaldehyde for 15 min. Cells were counterstained in DAPI mounting medium (Vecta Labs). The number of bacteria per infected BMM was counted and at least 200 infected BMMs of each genotype were counted in each of the three independent experiments.

To visualize the formation of the ASC speck in primary BMMs, cells were infected with *S.* Typhimurium strain SL1344 for 5, 10 and 20 min. BMMs were washed twice with PBS, fixed in 4% (wt/vol) paraformaldehyde for 15 min. Blocking was performed using 10% (vol/vol) normal goat serum (Dako) in 0.1% saponin (wt/vol) (Sigma) for 1 h. Cells were stained with a rabbit anti-ASC antibody (1:500 dilution, AL177, AG-25B-0006-C100, Adipogen) for 40 min followed by Alexa Fluor 568 anti-rabbit (1:250 dilution, Life Technologies) for 50 min. Cells were

counterstained in DAPI mounting medium (Vecta Labs). Cells were visualized and imaged using a Leica DM6000 B fluorescence microscope.

For phalloidin staining and 3D reconstruction, immortalized BMMs were detached using Accutase solution (Sigma) and seeded onto glass bottomed well chambers in serum limiting DMEM for 4 h. Supernatant was aspirated and *S.* Typhimurium JH3016 (MOI 10) was added. After 5 min, samples were aspirated and washed with PBS, fixed with 4% (wt/vol) paraformaldehyde for 10 min, blocked with 5% (wt/vol) BSA for 60 min, and stained with anti-*Salmonella* O antigen antibody (1:1,000 dilution, R30956901, Remel, ThermoScientific) for 60 min. Samples were washed with PBS and stained with Alexa Fluor 488 anti-rabbit IgG (1:1,000 dilution, Life Technologies) and phalloidin-568 (1:50 dilution, Life Technologies) for 60 min. Samples were washed with PBS three times and mounted with DAPI mounting medium (Vecta Labs). Samples were imaged on the Leica SP5 laser scanning confocal microscope (63×, 1.4NA) and analyzed using LAS AF software (Leica).

Optical Stretcher. We used a microfluidic optical stretcher – a specific dual-beam optical trap capable of inducing well-defined stresses on whole single cells in suspension – to measure the overall deformability and creep compliance of cells (29, 30, 39).

Detailed information is presented in SI Materials and Methods.

ACKNOWLEDGEMENTS

We would like to thank K.A. Fitzgerald (University of Massachusetts Medical School, USA) and E. Creagh (Trinity College Dublin) for supplying the knockout mouse strains. Financial support

for this work was provided by a Cambridge International Scholarship (to S.M.M.), European Research Council Starting Investigator Grant "LightTouch" 282060 (to J.R.G.), Biotechnology and Biological Sciences Research Council (BBSRC) Grants BB/H003916/1 and BB/K006436/1 and BBSRC Research Development Fellowship BB/ H021930/1 (to C.E.B.)

REFERENCES

1. Crump JA, Luby SP, & Mintz ED (2004) The global burden of typhoid fever. *Bull World Health Organ* 82(5):346-353.
2. Aderem A & Underhill DM (1999) Mechanisms of phagocytosis in macrophages. *Annual review of immunology* 17:593-623.
3. Mastroeni P, Grant A, Restif O, & Maskell D (2009) A dynamic view of the spread and intracellular distribution of *Salmonella enterica*. *Nature reviews. Microbiology* 7(1):73-80.
4. Fields PI, Swanson RV, Haidaris CG, & Heffron F (1986) Mutants of Salmonella typhimurium that cannot survive within the macrophage are avirulent. *Proceedings of the National Academy of Sciences of the United States of America* 83(14):5189-5193.
5. Haraga A, Ohlson MB, & Miller SI (2008) Salmonellae interplay with host cells. *Nature reviews. Microbiology* 6(1):53-66.
6. Janeway CA, Jr. & Medzhitov R (2002) Innate immune recognition. *Annual review of immunology* 20:197-216.
7. Tschopp J, Martinon F, & Burns K (2003) NALPs: a novel protein family involved in inflammation. *Nat Rev Mol Cell Biol* 4(2):95-104.
8. Zhao Y*, et al.* (2011) The NLRC4 inflammasome receptors for bacterial flagellin and type III secretion apparatus. *Nature* 477(7366):596-600.
9. Kofoed EM & Vance RE (2011) Innate immune recognition of bacterial ligands by NAIPs determines inflammasome specificity. *Nature* 477(7366):592-595.
10. Yang J, Zhao Y, Shi J, & Shao F (2013) Human NAIP and mouse NAIP1 recognize bacterial type III secretion needle protein for inflammasome activation. *Proceedings of the National Academy of Sciences of the United States of America* 110(35):14408-14413.
11. Rayamajhi M, Zak DE, Chavarria-Smith J, Vance RE, & Miao EA (2013) Cutting Edge: Mouse NAIP1 Detects the Type III Secretion System Needle Protein. *J Immunol* 191(8):3986-3989.
12. Mariathasan S*, et al.* (2004) Differential activation of the inflammasome by caspase-1 adaptors ASC and Ipaf. *Nature* 430(6996):213-218.
13. Broz P, von Moltke J, Jones JW, Vance RE, & Monack DM (2010) Differential requirement for Caspase-1 autoproteolysis in pathogen-induced cell death and cytokine processing. *Cell host & microbe* 8(6):471-483.
14. Kayagaki N*, et al.* (2011) Non-canonical inflammasome activation targets caspase-11. *Nature* 479(7371):117-121.
15. Broz P*, et al.* (2012) Caspase-11 increases susceptibility to *Salmonella* infection in the absence of caspase-1. *Nature* 490(7419):288-291.
16. Gurung P*, et al.* (2012) Toll or Interleukin-1 Receptor (TIR) Domain-containing Adaptor Inducing Interferon-beta (TRIF)-mediated Caspase-11 Protease Production Integrates Toll-like Receptor 4 (TLR4) Protein- and Nlrp3 Inflammasome-mediated Host Defense against Enteropathogens. *The Journal of biological chemistry* 287(41):34474-34483.
17. Man SM*, et al.* (2014) Inflammasome activation causes dual recruitment of NLRC4 and NLRP3 to the same macromolecular complex. *Proceedings of the National Academy of Sciences of the United States of America* 111(20):7403-7408.

18. Miao EA, *et al.* (2010) Caspase-1-induced pyroptosis is an innate immune effector mechanism against intracellular bacteria. *Nature immunology* 11(12):1136-1142.
19. Franchi L, *et al.* (2012) NLRC4-driven production of IL-1beta discriminates between pathogenic and commensal bacteria and promotes host intestinal defense. *Nature immunology* 13(5):449-456.
20. Sellin ME, *et al.* (2014) Epithelium-Intrinsic NAIP/NLRC4 Inflammasome Drives Infected Enterocyte Expulsion to Restrict *Salmonella* Replication in the Intestinal Mucosa. *Cell host & microbe* 16(2):237-248.
21. Gog JR, *et al.* (2012) Dynamics of *Salmonella* infection of macrophages at the single cell level. *J R Soc Interface* 9(75):2696-2707.
22. West AP, *et al.* (2011) TLR signalling augments macrophage bactericidal activity through mitochondrial ROS. *Nature* 472(7344):476-480.
23. Hicks SW & Galan JE (2013) Exploitation of eukaryotic subcellular targeting mechanisms by bacterial effectors. *Nature reviews. Microbiology* 11(5):316-326.
24. Brenner SL & Korn ED (1980) The effects of cytochalasins on actin polymerization and actin ATPase provide insights into the mechanism of polymerization. *The Journal of biological chemistry* 255(3):841-844.
25. Brenner SL & Korn ED (1979) Substoichiometric concentrations of cytochalasin D inhibit actin polymerization. Additional evidence for an F-actin treadmill. *The Journal of biological chemistry* 254(20):9982-9985.
26. Poyet JL, *et al.* (2001) Identification of Ipaf, a human caspase-1-activating protein related to Apaf-1. *The Journal of biological chemistry* 276(30):28309-28313.
27. Proell M, Gerlic M, Mace PD, Reed JC, & Riedl SJ (2013) The CARD plays a critical role in ASC foci formation and inflammasome signalling. *Biochem J* 449(3):613-621.
28. Man SM, *et al.* (2013) *Salmonella* infection induces recruitment of Caspase-8 to the inflammasome to modulate IL-1beta production. *J Immunol* 191(10):5239-5246.
29. Guck J, *et al.* (2001) The optical stretcher: a novel laser tool to micromanipulate cells. *Biophys. J.* 81(2):767-784.
30. Lautenschläger F, *et al.* (2009) The regulatory role of cell mechanics for migration of differentiating myeloid cells. *Proceedings of the National Academy of Sciences of the United States of America* 106(37):15696-15701.
31. Guck J, Lautenschläger F, Paschke S, & Beil M (2010) Critical review: cellular mechanobiology and amoeboid migration. *Integrative biology : quantitative biosciences from nano to macro* 2(11-12):575-583.
32. Chen KW, *et al.* (2014) The neutrophil NLRC4 inflammasome selectively promotes IL-1beta maturation without pyroptosis during acute *Salmonella* challenge. *Cell reports* 8(2):570-582.
33. Lamkanfi M, *et al.* (2008) Targeted peptidecentric proteomics reveals caspase-7 as a substrate of the caspase-1 inflammasomes. *Mol Cell Proteomics* 7(12):2350-2363.
34. Konradt C, *et al.* (2011) The *Shigella flexneri* type three secretion system effector IpgD inhibits T cell migration by manipulating host phosphoinositide metabolism. *Cell host & microbe* 9(4):263-272.
35. Salgado-Pabon W, *et al.* (2013) *Shigella* impairs T lymphocyte dynamics in vivo. *Proceedings of the National Academy of Sciences of the United States of America* 110(12):4458-4463.
36. Willingham SB, *et al.* (2007) Microbial pathogen-induced necrotic cell death mediated by the inflammasome components CIAS1/cryopyrin/NLRP3 and ASC. *Cell host & microbe* 2(3):147-159.
37. Suzuki T, *et al.* (2007) Differential regulation of caspase-1 activation, pyroptosis, and autophagy via Ipaf and ASC in *Shigella*-infected macrophages. *PLoS pathogens* 3(8):e111.
38. Hautefort I, Proenca MJ, & Hinton JC (2003) Single-copy green fluorescent protein gene fusions allow accurate measurement of *Salmonella* gene expression in vitro and during infection of mammalian cells. *Applied and environmental microbiology* 69(12):7480-7491.
39. Guck J, *et al.* (2005) Optical deformability as an inherent cell marker for testing malignant transformation and metastatic competence. *Biophys. J.* 88(5):3689-3698.

FIGURE LEGENDS

Fig. 1. The NLRC4–Caspase-1 axis restricts high levels of intracellular *S.* Typhimurium numbers in macrophages. (A) Unprimed primary bone marrow-derived macrophages (BMMs) were infected with *S.* Typhimurium (MOI 1) for 1 h. Following 1 h infection, BMMs were treated with gentamicin (50 μg/ml) for 1 h to kill extracellular bacteria. Host cell lysates were plated onto LB agar and the number of viable intracellular bacteria was enumerated. (B) Unprimed BMMs were infected with *S.* Typhimurium expressing green fluorescent protein (MOI 10) for 1 h, followed by gentamicin treatment (50 μg/ml) for 1 h to kill extracellular bacteria. The percentages of BMMs harboring different number of bacteria were determined by microscopy (WT, n=1,134; *Nlrc4*$^{-/-}$, n=765; *Casp1/11*$^{-/-}$, n=708; *Nlrp3*$^{-/-}$ n=663; *Asc*$^{-/-}$, n=731). (C) Unprimed BMMs were infected with *ΔfliCΔfljBΔprgJ S.* Typhimurium (MOI 1) for 1 h and the number of viable intracellular bacteria was enumerated. Data are the mean of three independent experiments and error bars represent s.e.m. (A) One-way ANOVA with a Dunnett's multiple comparisons test. (C) Two-way ANOVA with a Tukey's multiple comparisons test. ***$P < 0.001$; ns, no statistical significance.

Fig. 2. NLRC4 regulates mitochondrial ROS and H_2O_2 production to restrict bacterial replication by *Salmonella* in the *Salmonella*-containing vacuole (SCV). (A) The bacterial growth rate in each SCV was determined in WT and *Nlrc4*$^{-/-}$ BMDMs using live confocal imaging of SCVs (WT, n=11; *Nlrc4*$^{-/-}$ n=30) over 17 h following inoculation. The growth rate of *S.* Typhimurium was calculated using the formula Δn/T, where Δn is the number of bacteria in a SCV immediately prior to the death of a macrophage minus the number of bacteria following the formation of a SCV, and T is the length of time that the macrophage had survived over the

course of the infection. (B,C) Unprimed BMMs were infected with *S.* Typhimurium (MOI 10) for 30 min and stained with MitoSOX stain or CM-H_2DCFDA for 30 min. (B) The levels of mROS and (C) H_2O_2 were measured using flow cytometry. (D) WT BMMs were treated with *N*-Acetyl-L-cysteine (NAC) for 1.5 h and then infected with *S.* Typhimurium (MOI 1) for 1 h, followed by gentamicin treatment for a total of 2 or 6 h. Lysates from BMMs were plated on LB agar and the number of viable intracellular bacteria was enumerated. Data are representative of three (C, D) or four (B) independent experiments. Error bars indicate s.e.m. *t*-test (two-tailed), **P*<0.05; ***P*<0.01;

Fig. 3. NLRC4 inflammasome functions are linked to the actin cytoskeleton.

(A) Unprimed BMMs were infected with *S.* Typhimurium expressing green fluorescent protein (MOI 10) and tracked by confocal live imaging for 1 h. The number of bacteria internalized into each macrophage was counted every 60 s. (B) The number of viable intracellular bacteria recovered from WT BMMs infected with *S.* Typhimurium in the presence of the vehicle control DMSO, cytochalasin D (0.2, 2, and 20 μM) or colchicine (1, 10 and 100 μM) was counted. (C) Host cell viability of and (D) levels of IL-1β secreted from LPS-primed WT BMMs infected with *S.* Typhimurium for 1 h in the presence of the vehicle control DMSO, cytochalasin D or colchicine. (E) Unprimed WT BMMs were infected with *S.* Typhimurium for 1 h and stained for ASC (red) and DNA (blue). Data are the mean of three independent experiments and error bars represent s.e.m. One-way ANOVA with a Dunnett's multiple comparisons test. **P*<0.05; ***P*<0.01; ****P*<0.001; *****P*<0.0001; ns, not statistically significant.

Fig. 4. NLRC4 activation induces physical stiffening of macrophages by limiting actin availability for bacterial uptake and impairs bacterial dissemination. (A) The principle and

setup of the optical stretcher. Two diverging and counter-propagating laser beams emanating from single-mode optical fibres are used to trap and deform single suspended cells. A 50:50-intensity-ratio fibre coupler (FC) is used to split the output of a fibre laser into the two optical fibres. A personal computer (PC) is used for laser control and data acquisition by video microscopy via a CCD camera. (B) Unprimed primary BMMs were infected with GFP-expressing *S.* Typhimurium (MOI 10) for 10 min. BMMs were then serially trapped and stretched outwardly along the laser beam axis. Shown are (left) the average creep compliance responses of the various cells during the 4 seconds of stretching (indicated by darker red) and (right) box plots of the average compliance during the stretch. (C) 3D reconstruction of phalloidin-stained F-actin cytoskeleton (red) in unprimed immortalized BMMs infected with GFP-expressing *S.* Typhimurium (MOI of 10) for 5 min. (D) Unprimed primary BMMs were imaged for 3 h and then infected with *S.* Typhimurium (MOI 10) and imaged for 30 min. For each cell the movies were divided in sections of 10 min and cell movement was analyzed. Data shown are from uninfected cells (over the 3 h time period) and from cells infected with *S.* Typhimurium for 20 to 30 min. The mean square displacement ($MSD(\tau) = \langle (x(t+\tau) - x(t))^2 \rangle_t$) of infected cells compared to uninfected cells (τ = 2 to 10 min) is fitted with a power law $D_{eff} \cdot t^{\alpha}$. From the resulting fit the value of the MSD at 5 min is calculated. In the box plot, the red bars represent the median of the distribution, the blue edges of the box indicate the 25th and 75th percentile, and dashed bars indicate the extreme points. (E) Histopathology of livers from WT (n=4) and *Nlrc4*$^{-/-}$ (n=5) mice intravenously infected with *S.* Typhimurium for 7 days. Dashed circles indicate extent of lesions. (F) Livers were fixed and lesions were counted from four liver sections from each mouse. *t*-test (two-tailed), ***P<0.001; ****P<0.0001; ns, not statistically significant.

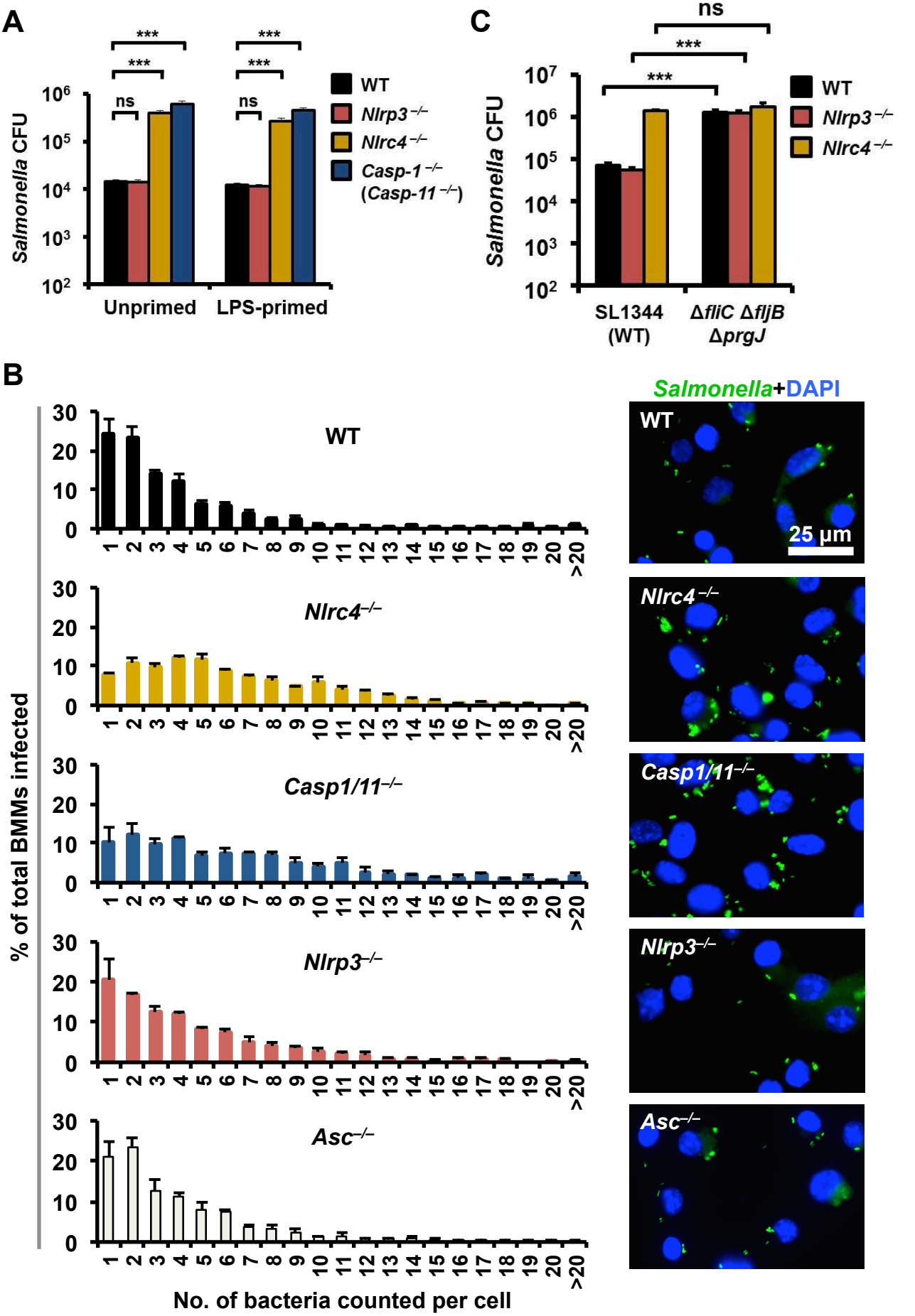
A
Salmonella CFU
10^6
10^5
10^4
10^3
10^2
***
***
***
***
ns
ns
WT
Nlrp3 −/−
Nlrc4 −/−
Casp-1 −/−
(Casp-11 −/−)
Unprimed
LPS-primed
C
ns
***
***
Salmonella CFU
10^7
10^6
10^5
10^4
10^3
10^2
WT
Nlrp3 −/−
Nlrc4 −/−
SL1344
(WT)
ΔfliC ΔfljB
ΔprgJ
B
% of total BMMs infected
WT
Nlrc4−/−
Casp1/11−/−
Nlrp3−/−
Asc−/−
30
20
10
0
1 2 3 4 5 6 7 8 9 10 11 12 13 14 15 16 17 18 19 20 >20
No. of bacteria counted per cell
Salmonella+DAPI
WT
25 μm
Nlrc4 −/−
Casp1/11−/−
Nlrp3−/−
Asc−/−

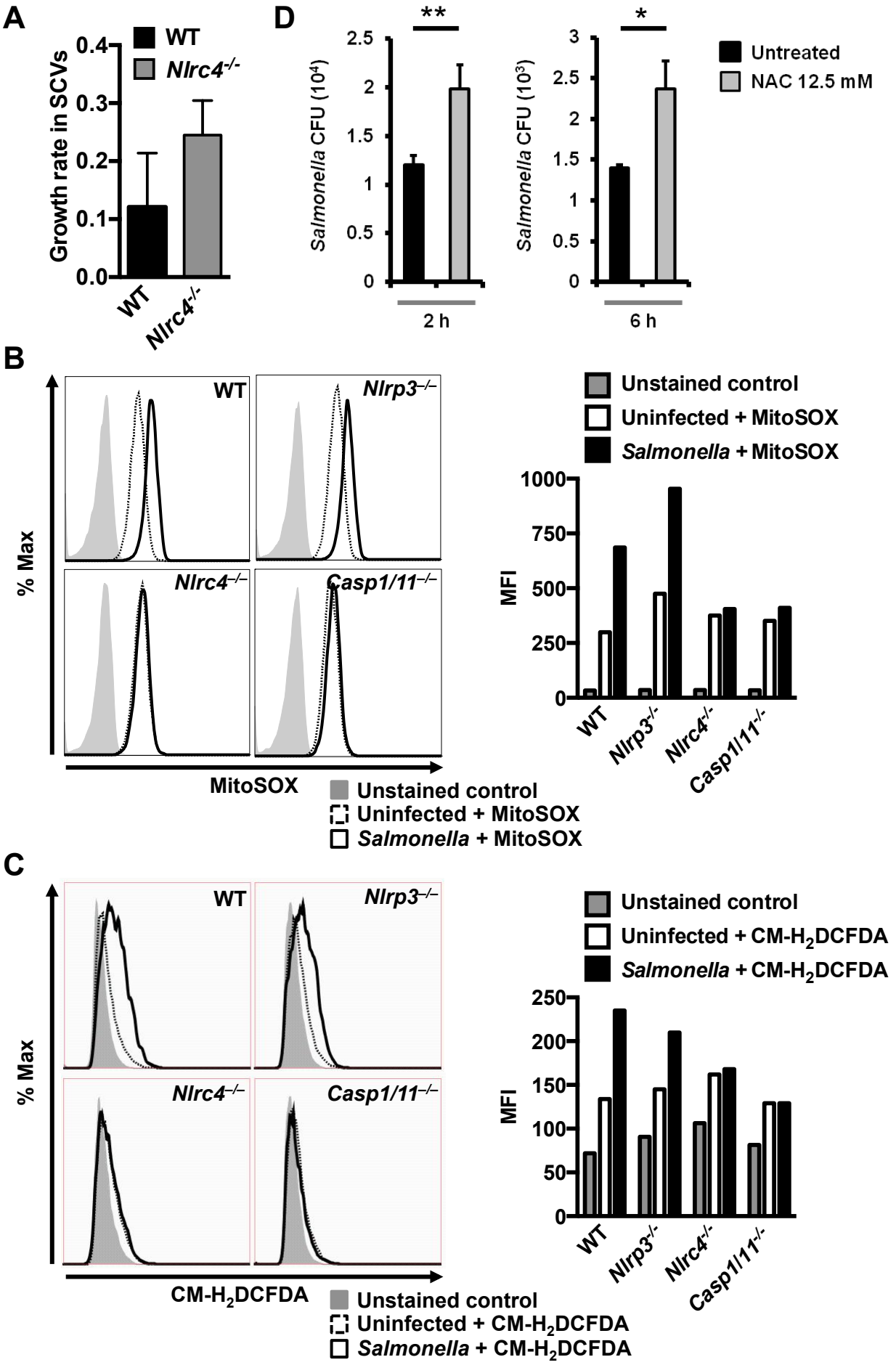
A
WT
Nlrc4-/-
Growth rate in SCVs
0.4
0.3
0.2
0.1
0.0
WT
Nlrc4-/-
D
**
*
Salmonella CFU (10^4)
Salmonella CFU (10^3)
2.5
2
1.5
1
0.5
0
3
2.5
2
1.5
1
0.5
0
2 h
6 h
Untreated
NAC 12.5 mM
B
WT
Nlrp3-/-
Nlrc4-/-
Casp1/11-/-
% Max
MitoSOX
Unstained control
Uninfected + MitoSOX
Salmonella + MitoSOX
MFI
1000
750
500
250
0
WT
Nlrp3-/-
Nlrc4-/-
Casp1/11-/-
C
WT
Nlrp3-/-
Nlrc4-/-
Casp1/11-/-
% Max
CM-H2DCFDA
Unstained control
Uninfected + CM-H2DCFDA
Salmonella + CM-H2DCFDA
MFI
250
200
150
100
50
0
WT
Nlrp3-/-
Nlrc4-/-
Casp1/11-/-

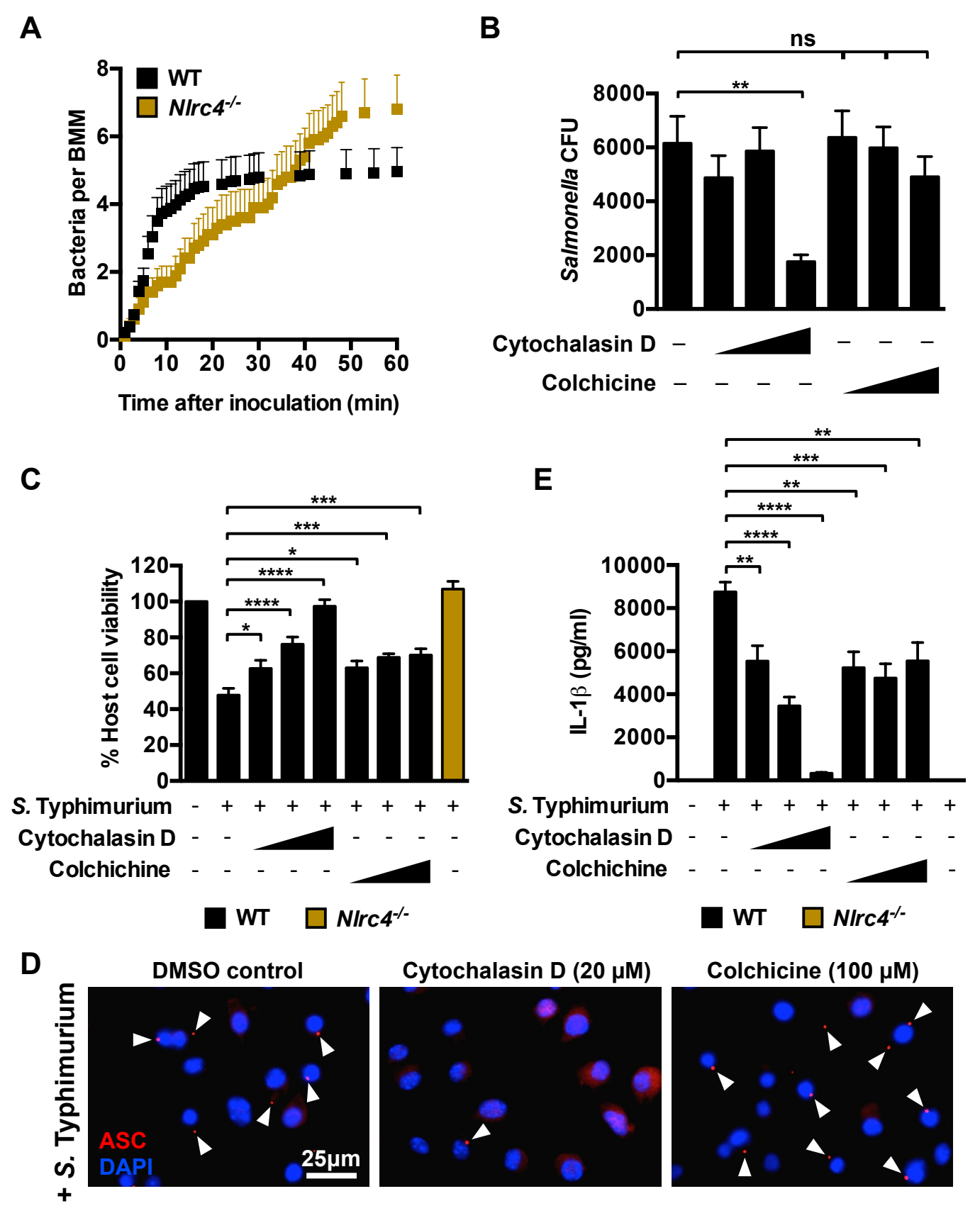
A
WT
Nlrc4-/-
Bacteria per BMM
Time after inoculation (min)
B
ns
**
Salmonella CFU
Cytochalasin D
Colchicine
C
% Host cell viability
S. Typhimurium
Cytochalasin D
Colchicine
WT
Nlrc4-/-
E
IL-1β (pg/ml)
S. Typhimurium
Cytochalasin D
Colchicine
WT
Nlrc4-/-
D
DMSO control
Cytochalasin D (20 μM)
Colchicine (100 μM)
+ S. Typhimurium
ASC
DAPI
25μm

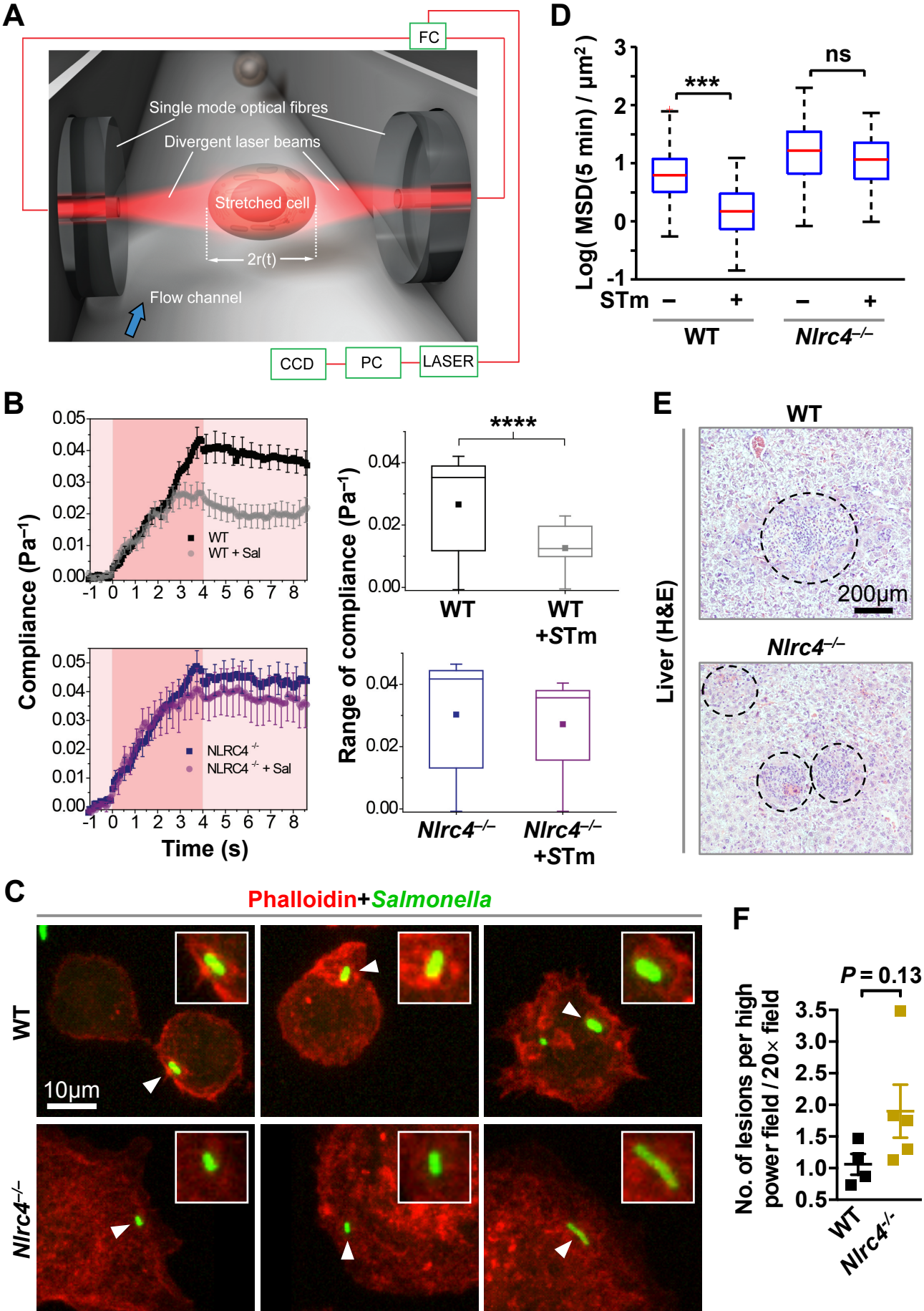
A
FC
Single mode optical fibres
Divergent laser beams
Stretched cell
2r(t)
Flow channel
CCD
PC
LASER
D
Log(MSD(5 min) / μm²)
***
ns
STm
WT
Nlrc4−/−
B
Compliance (Pa⁻¹)
WT
WT + Sal
NLRC4 -/-
NLRC4 -/- + Sal
Time (s)
****
Range of compliance (Pa⁻¹)
WT
WT +STm
Nlrc4−/−
Nlrc4−/− +STm
E
Liver (H&E)
WT
Nlrc4−/−
200μm
C
Phalloidin+Salmonella
WT
Nlrc4−/−
10μm
F
P = 0.13
No. of lesions per high power field / 20× field
WT
Nlrc4-/-